Journal of Theoretical and Applied Information Technology
30th April 2024. Vol.102. No 8

ISSN: 1992-8645 www.jatit.org E-ISSN: 1817-3195

EXACT QUANTUM STATE COMPUTATION IN QUANTUM PHASE ESTIMATION

EUN-JIN IM[1]

[1]Professor, Kookmin University, School of Software, Seoul, Korea

E-mail: [1]ejim@kookmin.ac.kr

ABSTRACT

Quantum phase estimation is a fundamental algorithm in quantum computing for estimating the phase of an eigenvalue for a unitary operator. While the output state of quantum phase estimation circuit exactly matches to the phase represented as rational number with denominator as powers of 2, the measurement could be read in many different states for phases outside this form. In this paper, we address this gap by formulating and precisely computing the quantum state of QPE when the phase is not exactly represented as a rational number with a denominator in a power of 2. Leveraging mathematical techniques from number theory and trigonometry, we derive explicit expressions for the quantum state of QPE in these cases. To validate our results, we compare our theoretical predictions with simulations using the Qiskit framework, confirming the accuracy of our formulations. Our findings provide insights into the behavior of QPE for phases, expanding the understanding and applicability of this fundamental quantum algorithm.

Keywords: *Quantum Phase Estimation, Quantum Fourier Transform, Shor's algorithm, Probability Distribution, Quantum State*

1. INTRODUCTION

Quantum phase estimation (QPE) stands as a foundational algorithm in quantum computing, essential for estimating the phase of unitary operators with high precision. Originally introduced by Kitaev [1], QPE has garnered significant attention for its role in various quantum algorithms, including Shor's algorithm for factoring large integers [2][3][4] and broad range of quantum simulation techniques [5][6][7]. Conventionally, QPE is well-understood when the phase is represented as a rational number with the denominator in a power of 2, allowing for efficient quantum circuit implementations. However, the behavior of QPE for phases outside this conventional form remains less explored, posing challenges for understanding and leveraging the algorithm in practical quantum computations.

In this paper, we address this gap by formulating and precisely computing the quantum state of QPE when the phase is not exactly represented as a rational number with a denominator in a power of 2. Representation of output state of QPE in such cases is not explicitly formulated in any previous literature. Building upon mathematical techniques from number theory and trigonometry, our result shows that the probability of a state closest to the approximation is highest in these cases. Our formulations provide a comprehensive understanding of QPE's behavior for phases beyond the conventional rational representations, offering insights into its theoretical foundations and practical implications.

To validate our theoretical results, we employ simulations using the Qiskit framework [10], a leading platform for quantum computing research and development. By comparing our theoretical predictions with Qiskit simulations, we confirm the accuracy and efficacy of our formulations, establishing their utility in practical quantum computations. Our findings not only extend the understanding of QPE but also pave the way for exploring its applications in scenarios where phases are not strictly rational with denominators in powers of 2.

2. QUANTUM PHASE ESTIMATION

Given an n-qubit quantum gate U, Figure 1 shows a circuit diagram implementing Quantum Phase Estimation for gate U. Throughout this paper in the circuit diagram, we will use a convention of numbering qubit subscripts from bottom to top, which means that bottom-most qubit represents the highest bit when the measured state is interpreted as a binary number. We will name qubits with prefix q as in qx_i in order to represent the position of the

Journal of Theoretical and Applied Information Technology
30th April 2024. Vol.102. No 8

ISSN: 1992-8645 www.jatit.org E-ISSN: 1817-3195

qubit in the quantum circuit, where x_i represent the state of the qubit. In the QPE circuit, the bottom t qubits will be measured, and the phase is estimated based on the measurement. When Dirac notation [11] is used to describe quantum operation, the bottom qubit is located to the left of the top qubit.

H represent a Hadamard gate, whose quantum operation is described with a matrix $\begin{pmatrix} \frac{1}{\sqrt{2}} & \frac{1}{\sqrt{2}} \\ \frac{1}{\sqrt{2}} & -\frac{1}{\sqrt{2}} \end{pmatrix}$. For an n-qubit quantum gate U whose operation is described with a $2^n \times 2^n$ matrix U, U^k represents an n-qubit quantum gate whose operation is described with a matrix U^k. U gate connected to a qubit using a vertical line and a black dot represents a controlled-U gate, $cU_{qx_i,qy}$, where the control qubit is qx_i qubit and the target qubits are qys. The operation of this $(n+1)$-qubit gate $cU_{qx_i,qy}$ is as follows.

$$cU_{qxi,qy}|x_i\rangle|y\rangle = \begin{cases} |x_i\rangle|y\rangle, & \textbf{for } |x_i\rangle = |0\rangle \\ |x_i\rangle U|y\rangle, & \textbf{for } |x_i\rangle = |1\rangle \end{cases}$$

As derived in [12][13] the inverse Quantum Fourier Transform circuit, denoted as $QFT^\dagger$, transforms the input state to the output state as in the following.

$$QFT^\dagger|x_{t-1}x_{t-2}\dots x_1x_0\rangle = \frac{|0\rangle + e^{-2\pi i\frac{x_0}{2^1}}|1\rangle}{\sqrt{2}} \otimes \frac{|0\rangle + e^{-2\pi i\left(\frac{x_1}{2^1}+\frac{x_0}{2^2}\right)}|1\rangle}{\sqrt{2}} \otimes \dots \otimes \frac{|0\rangle + e^{-2\pi i\left(\frac{x_{t-1}}{2^1}+\frac{x_{t-2}}{2^2}+\dots+\frac{x_0}{2^t}\right)}|1\rangle}{\sqrt{2}}$$

If the state of qx qubits is measured along the z-axis as $x = x_{t-1}x_{t-2}\dots x_1x_0 \in \{0,1\}^t$, $\lambda = \frac{x}{2^t}$ is a phase of eigenvalue of U, which satisfies $U|\psi\rangle = e^{2\pi i\theta}|\psi\rangle$ for some eigenvector $|\psi\rangle$ of U.

For example, if $\lambda = \frac{1}{8}$, the probability distribution of measurement of QPE circuit with $t=3$ qubits is as in Figure 2. In the case when the denominator of λ is 2^t, the output state is $|1\rangle$ with probability = 1, theoretically.

If $\lambda = \frac{1}{3}$,where the denominator of λ is not represented as 2^t, the probability distribution of measurement is as shown in Figure 3. We formulate the probability distribution in the following section.

3. ANALYSIS OF QPE MEASUREMENT

By the definition of a controlled-U gate, if we apply a controlled-U gate, $cU_{qx_i,qy}$, to an arbitrary quantum state $|x_i\rangle = \alpha|0\rangle + \beta|1\rangle$ and $|y\rangle = |\psi\rangle$, an eigenstate of U, the quantum state evolves to the following equation, for an eigenvalue, $e^{2\pi\lambda i}$.

$$\begin{aligned} cU_{qx_i,qy}|x_i\rangle|\psi\rangle &= \alpha|0\rangle|\psi\rangle + \beta|1\rangle U|\psi\rangle \\ &= \alpha|0\rangle|\psi\rangle + \beta|1\rangle e^{2\pi\lambda i}|\psi\rangle \\ &= (\alpha|0\rangle + \beta\, e^{2\pi\lambda i}|1\rangle)\,|\psi\rangle \end{aligned}$$

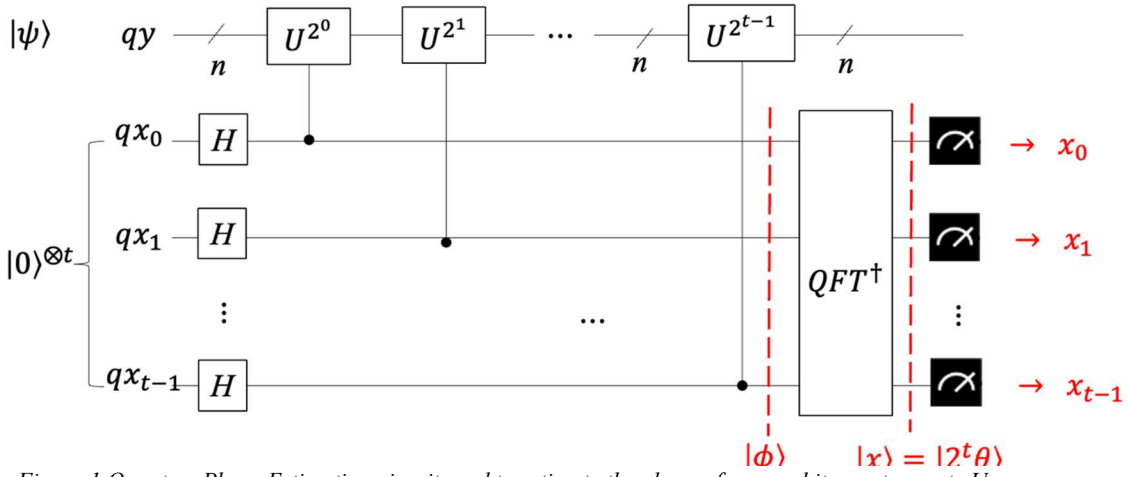

Figure 1 Quantum Phase Estimation circuit used to estimate the phase of an n-qubit quantum gate U

The result of this operation changes the quantum state of the control qubit when the initial state of the target qubit was an eigenstate of *U*. This operation is referred as a phase-kickback and used as a common technique for measuring operators in quantum error correcting codes, such as the surface code [14]. The circuit in Figure 1 makes use of the phase-kickback.

Following the equation,

$$\begin{aligned} U^{2^k}|y\rangle &= U^{2^k-1}\,\mathrm{U}|y\rangle \\ &= U^{2^k-1}\,e^{2\pi\lambda i}|y\rangle \\ &= U^{2^k-2}Ue^{2\pi\lambda i}|y\rangle \\ &= U^{2^k-2}\,e^{2\pi 2\lambda i}|y\rangle \\ &= \cdots \\ &= U^0 e^{2\pi 2^k\lambda i}|y\rangle \\ &= e^{2\pi 2^k\lambda i}|y\rangle \end{aligned}$$

$|\psi\rangle$, an eigenstate of *U*, is also an eigenstate of U^{2^k} for eigenvalue $e^{2\pi 2^k\lambda i}$.

The operation of the controlled-$U^{2^k}_{qx_i,qy}$ gate is described as in the following.

$$cU^{2^k}{}_{qxi,qy}|x_i\rangle|y\rangle = \begin{cases} |x_i\rangle|y\rangle, & \textbf{for } |x_i\rangle = |0\rangle \\ |x_i\rangle U^{2^k}|y\rangle = e^{2\pi 2^k\lambda i}|x_i\rangle|y\rangle, & \textbf{for } |x_i\rangle = |1\rangle \end{cases}$$

This implies that he role of the controlled-U^{2^k} is to change the state of control qubit, which is one of $qx_0, qx_1, \ldots, qx_{t-1}$ qubits in the circuit in Figure 1.

The initial state of the circuit is prepared as $|0\rangle^{\otimes t}|\psi\rangle$ where $|\psi\rangle$ is an eigenstate of *U*. Hadamard gates *H* changes the quantum states of qx_i s $|0\rangle \to |+\rangle = \frac{1}{\sqrt{2}}(|0\rangle + |1\rangle)$ .Thus, the quantum state $|\phi\rangle$ which includes only bottom *t* qubits, $qx_{t-1}, \ldots, qx_0$, is represented as the following equation.

$$\begin{aligned} |\phi\rangle &= \frac{|0\rangle + e^{2\pi\lambda i 2^{t-1}}|1\rangle}{\sqrt{2}} \otimes \frac{|0\rangle + e^{2\pi\lambda i 2^{t-2}}|1\rangle}{\sqrt{2}} \otimes \\ &\ldots \otimes \frac{|0\rangle + e^{2\pi\lambda i 2^{1}}|1\rangle}{\sqrt{2}} \otimes \frac{|0\rangle + e^{2\pi\lambda i 2^{0}}|1\rangle}{\sqrt{2}} \\ &= \frac{1}{2^t}\sum_{x\in\{0,1\}^t} e^{2\pi i\lambda(2^{t-1}x_{t-1}+\cdots+2^0x_0)}\,|x_{t-1}\ldots x_1x_0\rangle \end{aligned}$$

using the representation

$$|0\rangle + e^{2\pi\lambda i 2^k}|1\rangle = \sum_{x\in\{0,1\}} e^{2\pi\lambda i 2^k x}|x\rangle.$$

The inverse Quantum Fourier Transform circuit, denoted as $QFT^\dagger$, transforms the input state to the output state and the state is rewritten as in the following equation.

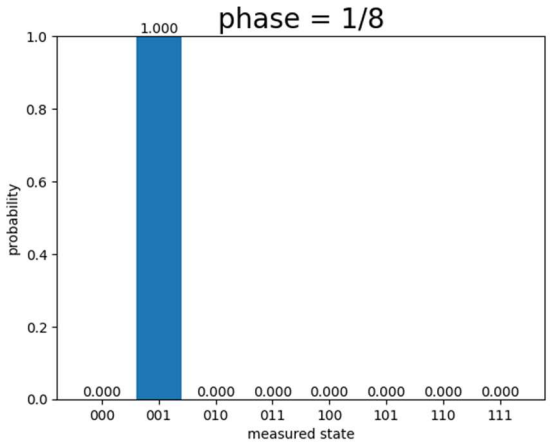

Figure 2 Probability Distribution of Measurement in QPE Circuit for a Gate with Phase $\lambda = \frac{1}{8}$ USING 3 Measurement Qubits.

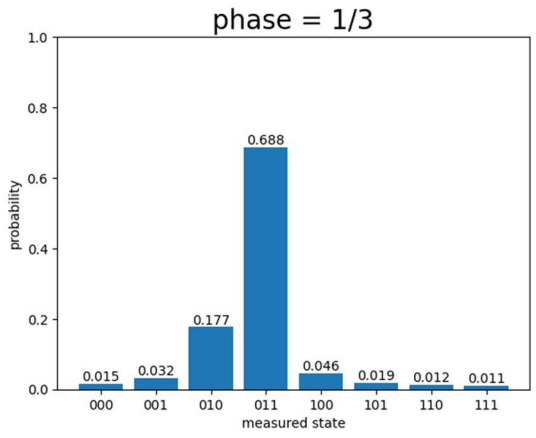

Figure 3 Probability Distribution of Measurement in QPE Circuit for a Gate with Phase $\lambda = \frac{1}{3}$ USING 3 Measurement Qubits.

$$QFT^{\dagger}|x_{t-1}x_{t-2}\dots x_1x_0\rangle$$
$$= \frac{|0\rangle + e^{-2\pi i\frac{x_0}{2^1}}|1\rangle}{\sqrt{2}} \otimes \frac{|0\rangle + e^{-2\pi i\left(\frac{x_1}{2^1}+\frac{x_0}{2^2}\right)}|1\rangle}{\sqrt{2}} \otimes$$
$$\dots \otimes \frac{|0\rangle + e^{-2\pi i\left(\frac{x_{t-1}}{2^1}+\frac{x_{t-2}}{2^2}+\dots+\frac{x_0}{2^t}\right)}|1\rangle}{\sqrt{2}}$$
$$= \frac{1}{\sqrt{2}} \sum_{y_{t-1}=0}^{1} e^{\frac{-2\pi i y_{t-1}x_0}{2}} |y_{t-1}\rangle \otimes$$
$$\frac{1}{\sqrt{2}} \sum_{y_{t-2}=0}^{1} e^{\frac{-2\pi i y_{t-2}(2x_1+x_0)}{2^2}} |y_{t-2}\rangle \otimes \dots$$
$$\frac{1}{\sqrt{2}} \sum_{y_0=0}^{1} e^{\frac{-2\pi i y_0(2^{t-1}x_{t-1}+\dots+2x_1+x_0)}{2^t}} |y_0\rangle$$
$$= \frac{1}{\sqrt{2^t}} \sum_{y\in\{0,1\}^t} e^{\frac{-2\pi i(y_{t-1}2^{t-1}x_0+\dots+y_0(2^{t-1}x_{t-1}+\dots+x_0)}{2^t}} |y\rangle$$

Then $QFT^{\dagger}|\phi\rangle$ is represented with $c(y)$,

$$QFT^{\dagger}|\phi\rangle$$
$$= \frac{1}{\sqrt{2^t}} \sum_{x\in\{0,1\}^t} e^{2\pi i\lambda(2^{t-1}x_{t-1}+\dots+2^0x_0)}\, QFT^{\dagger}|x\rangle$$
$$= \sum_{y\in\{0,1\}^t} c(y)\,|y\rangle$$

$c(y)$ as defined in Equation 1 below. $c(y)$ is the probability amplitude of measuring $|y\rangle$.

We define θ_k as

$$\theta_k \equiv (\lambda 2^k - (y_{t-1-k}2^{t-1} + \dots + y_m 2^{k+m} + \dots + y_0 2^k)/2^t)\pi$$
$$= (\lambda 2^k - \textstyle\sum_{m=0}^{t-1-k} y_m\, 2^{k+m}/2^t)\,\pi$$

to rewrite $c(y)$ as

$$c(y) = \frac{1}{2^t}\prod_{k=0}^{t-1}\sum_{x_k\in\{0,1\}} e^{2i\theta_k x_k} = \frac{1}{2^t}\prod_{k=0}^{t-1}\left(1+e^{2i\theta_k}\right)$$

using the following relation

$$1 + e^{2\theta i} = 1 + \cos 2\theta + i\sin 2\theta$$
$$= 1 + (2\cos^2\theta - 1) + 2i\sin\theta\cos\theta$$
$$= 2\cos\theta\,(\cos\theta + i\sin\theta)$$
$$= 2\cos\theta\, e^{\theta i}$$

The probability amplitude of $|y\rangle, c(y)$ is represented as a product of cosine values and exponential functions of pure imaginary numbers as in the following.

$$c(y) = \frac{1}{2^t}\prod_{k=0}^{t-1}\left(1+e^{2i\theta_k}\right) = \prod_{k=0}^{t-1}\cos\theta_k\, e^{\theta_k i}$$

Because the square of L2-norm of probability amplitude indicates the probability of the state is measured, and L2 norm of exponential function of a pure imaginary number is 1 by Euler's formula, probability of measuring $|\phi\rangle = |y\rangle$ is analytically computed as a square product of *t* cosine values as in the following equation.

$$P(|y\rangle) = \|c(y)\|^2 = \prod_{k=0}^{t-1}\cos^2\theta_k$$

For example, in QPE circuit of *U* gate with *t=3* qubits for measurement,

$$c(y) = \cos\theta_2\, e^{\theta_2 i}\cos\theta_1\, e^{\theta_1 i}\cos\theta_0\, e^{\theta_0 i}$$

$$c(y) = \frac{1}{2^t}\sum_{x\in\{0,1\}^t} e^{2\pi i\left(\lambda(2^{t-1}x_{t-1}+\dots+2^0x_0)-\left(y_{t-1}2^{t-1}x_0+\dots+y_0(2^{t-1}x_{t-1}+\dots+x_0)\right)/2^t\right)}$$
$$= \frac{1}{2^t}\prod_{k=0}^{t-1}\sum_{x_k\in\{0,1\}} e^{2i\theta_k x_k} \qquad (1)$$

Journal of Theoretical and Applied Information Technology
30th April 2024. Vol.102. No 8

ISSN: 1992-8645 www.jatit.org E-ISSN: 1817-3195

where

$$\theta_2 \equiv (2^2\lambda - y_0 2^2/2^3)\pi$$

$$\theta_1 \equiv \left(2^1\lambda - \sum_{m=0}^{1} y_m 2^{1+m}/2^3\right)\pi = (2^1\lambda - (y_0 2^1 + y_1 2^2)/2^3)\pi$$

$$\theta_0 \equiv \left(2^0\lambda - \sum_{m=0}^{2} y_m 2^m/2^3\right)\pi = (2^0\lambda - (y_0 2^0 + y_1 2^1 + y_2 2^2)/2^3)\pi$$

for *U* gate with phase $\lambda = \frac{1}{3}$, where $\lambda \neq \frac{k}{2^t}$ for any integer *k* with *t=3* qubits for measurement, Table 1 shows the probabilities, $\|c(y)\|^2$ along with $\theta_0, \theta_1, \theta_2$.

This result matches the graph in Figure 3. Because $\frac{1}{3}$ is close to $\frac{3}{8}$, the probability of measuring $|y\rangle = |011\rangle$ is highest and the probability decreases as the difference between *y* and $2^t\lambda$ increases.

Table 1 Probability of Measuring $|y\rangle$ in QPE Circuit for a Gate with Phase $\lambda = \frac{1}{3}$ Using 3 Measurement Qubits.

$\|y\rangle$	θ_0	θ_1	θ_2	Probability
$\|000\rangle$	$\frac{1}{3}\pi$	$\frac{2}{3}\pi$	$\frac{4}{3}\pi$	0.016
$\|001\rangle$	$\frac{5}{24}\pi$	$\frac{5}{12}\pi$	$\frac{5}{6}\pi$	0.032
$\|010\rangle$	$\frac{1}{12}\pi$	$\frac{1}{6}\pi$	$\frac{4}{3}\pi$	0.175
$\|011\rangle$	$-\frac{1}{24}\pi$	$-\frac{1}{12}\pi$	$\frac{5}{6}\pi$	0.688
$\|100\rangle$	$-\frac{1}{6}\pi$	$\frac{2}{3}\pi$	$\frac{4}{3}\pi$	0.047
$\|101\rangle$	$-\frac{7}{24}\pi$	$\frac{5}{12}\pi$	$\frac{5}{6}\pi$	0.019
$\|110\rangle$	$-\frac{5}{12}\pi$	$\frac{1}{6}\pi$	$\frac{4}{3}\pi$	0.013
$\|111\rangle$	$-\frac{13}{24}\pi$	$-\frac{1}{12}\pi$	$\frac{5}{6}\pi$	0.012

Let's take an example of the case when $\lambda = \frac{1}{8}$ where λ is a rational number with denominator as power of 2.

$$\theta_2 = (2^2/2^3 - y_0 2^2/2^3)$$
$$\theta_1 = (2^1/2^3 - (y_0 2^1 + y_1 2^2)/2^3)$$
$$\theta_0 = (2^0/2^3 - (y_0 2^0 + y_1 2^1 + y_2 2^2)/2^3)$$

Table 2 shows the probabilities, $\|c(y)\|^2$ along with $\theta_0, \theta_1, \theta_2$.

Table 2 Probability of Measuring $|y\rangle$ in QPE Circuit for a Gate with Phase $\lambda = \frac{1}{8}$ Using 3 Measurement Qubits.

$\|y\rangle$	θ_0	θ_1	θ_2	Probability
$\|000\rangle$	$\frac{1}{8}\pi$	$\frac{1}{4}\pi$	$\frac{1}{2}\pi$	0.000
$\|001\rangle$	0π	0π	0π	1.000
$\|010\rangle$	$-\frac{1}{8}\pi$	$-\frac{1}{4}\pi$	$\frac{1}{2}\pi$	0.000
$\|011\rangle$	$-\frac{1}{4}\pi$	$-\frac{1}{2}\pi$	0π	0.000
$\|100\rangle$	$-\frac{3}{8}\pi$	$\frac{1}{4}\pi$	$\frac{1}{2}\pi$	0.000
$\|101\rangle$	$-\frac{1}{2}\pi$	0π	0π	0.000
$\|110\rangle$	$-\frac{5}{8}\pi$	$-\frac{1}{4}\pi$	$\frac{1}{2}\pi$	0.000
$\|111\rangle$	$-\frac{3}{4}\pi$	$-\frac{1}{2}\pi$	0π	0.000

As the Table 2 illustrates, in the case when $\lambda = \frac{k}{2^k}$ for some integer *k*, θ_i for *c(k)* is represented as in the following.

$$\theta_i = \pi\left(2^i k/2^t - \sum_{m=0}^{t-1-i} k_m 2^{i+m}/2^t\right) = \pi\left(\sum_{m=0}^{t} 2^m k_m 2^i - \sum_{m=0}^{t-1-i} k_m 2^{i+m}\right)/2^t = \pi \sum_{m=t-i}^{t} 2^m k_m 2^i /2^t$$

$$= \pi \sum_{m'=0}^{i} 2^{m'+t} k_{m'+t-i} / 2^{t}$$
$$= \pi \sum_{m'=0}^{i} 2^{m'} k_{m'+t-i}$$

It is shown that all θ_i s of *c(k)* are integer multiples of π for some integer k when $\lambda = \frac{k}{2^k}$. Since $\cos^2 \theta_i = 1$, the probability of measuring $|k\rangle$ is 1, whereas the probability of measuring $|k'\rangle$ for $k' \neq k$ is 0. This result, shown in Table 2, is confirmed in the graph of Figure 2.

4. EVALUATION

The open-source quantum computing frameworks, such as IBM Qiskit [10] Google Cirq, Microsoft Q# and Rigetti Forest Quantum, has provided platforms for developing, simulating, and executing quantum algorithms [15].

We implement the QPE circuit using IBM Qiskit library as shown in Figure 4. The Qiskit circuit library provides *QFT* and *PhaseEstimation* classes implementing Quantum Fourier Transform and Quantum Phase Estimation. In this work, in order to illustrate the circuit composition, QPE circuit is composed of *H, U* gates and *QFT* class.

The Python code in Figure 4 shows the source code used to build and simulate the QPE circuit using Qiskit. IBM released a major update of Qiskit from v0.46.0 to v1.0.1 as of February 2024. The following code is written in the new version v1.0.1.

The circuit diagram of a quantum circuit built in the step 1 of Figure 4, is shown in Figure 5, generated using *QuantumCircuit.draw()* function.

The simulation result in step 3 of code in Figure 4 follows the probability distribution in Figure 3. The probability distribution confirms the computation in Table 1.

Modifying the variable *t* of code in Figure 4 from 3 to 4, we built a QPE circuit for *U* with phase $\frac{1}{3}$ for *t=4* measurement qubits, which increases precision in the measurement. The simulation exhibits the probability distribution in Figure 6.

```
# step 1 :
# build a phase estimation circuit with 'phase'
import numpy as np
from qiskit import QuantumCircuit, \
      QuantumRegister, ClassicalRegister
from qiskit.circuit.library import QFT

t = 3
n = 1
qx = QuantumRegister(t,'qx')
qy = QuantumRegister(n,'qy')
c = ClassicalRegister(t,'c')
qpe = QuantumCircuit(qy, qx, c)

phase = 1./3
qpe.x(qy)        # eigenstate |1>
qpe.barrier()
qpe.h(qx)
Un = 1
for qx_i in range(t):
  for i in range(Un):
    # controlled-Phase-Shift gate
     qpe.cp(2*np.pi*phase, qx[qx_i], qy);
  Un *= 2

qpe.compose(QFT(t,inverse=True), \
     range(n,n+t), inplace=True) \
     qpe.measure(range(n,n+t),range(t)))
 # depiction of a quantum circuit

qpe.draw(fold=-1, output='mpl')

# step 2 :
# simulate the circuit as many as 'shots' times
from qiskit.primitives.sampler import Sampler
sampler = Sampler()
job = sampler.run(qpe, shots=100000)
result = job.result()
prob = \
     result.quasi_dists[0].binary_probabilities()
print(prob)

# step 3 :
# visualize the probability of measurement
from qiskit.visualization \
     import plot_distribution
plot_distribution(prob)
```

Figure 4 Python Source Code simulating QPE Circuit for a Gate with Phase $\lambda = \frac{1}{3}$ Using 3 Measurement Qubits.

Journal of Theoretical and Applied Information Technology
30th April 2024. Vol.102. No 8

ISSN: 1992-8645 www.jatit.org E-ISSN: 1817-3195

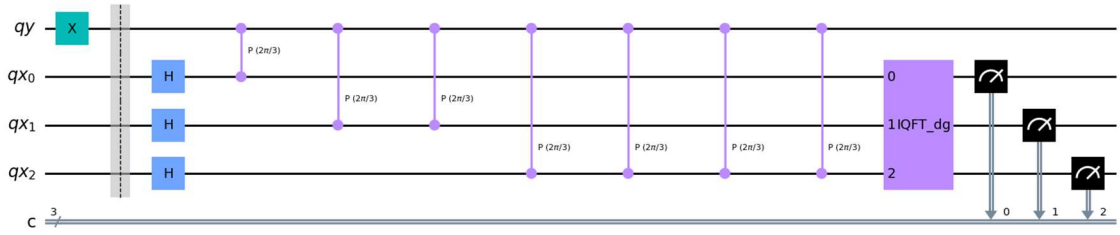

Figure 5 Qiskit drawing of QPE circuit with n=1, t=3

Table 3 Probability of Measuring y in QPE circuit for QPE Circuit for a Gate with Phase $\lambda = \frac{1}{3}$ Using 4 Measurement Qubits.

$\|y\rangle$	θ_0	θ_1	θ_2	θ_3	Computed Probability	Simulated Probability
$\|0000\rangle$	$\frac{1}{3}\pi$	$\frac{2}{3}\pi$	$\frac{4}{3}\pi$	$\frac{8}{3}\pi$	0.004	0.004
$\|0001\rangle$	$\frac{13}{48}\pi$	$\frac{13}{24}\pi$	$\frac{13}{12}\pi$	$\frac{13}{6}\pi$	0.005	0.005
$\|0010\rangle$	$\frac{5}{24}\pi$	$\frac{5}{12}\pi$	$\frac{5}{6}\pi$	$\frac{8}{3}\pi$	0.008	0.008
$\|0011\rangle$	$\frac{7}{48}\pi$	$\frac{7}{24}\pi$	$\frac{7}{12}\pi$	$\frac{13}{6}\pi$	0.015	0.015
$\|0100\rangle$	$\frac{1}{12}\pi$	$\frac{1}{6}\pi$	$\frac{4}{3}\pi$	$\frac{8}{3}\pi$	0.044	0.044
$\|0101\rangle$	$\frac{1}{48}\pi$	$\frac{1}{24}\pi$	$\frac{13}{12}\pi$	$\frac{13}{6}\pi$	0.685	0.685
$\|0110\rangle$	$-\frac{1}{24}\pi$	$-\frac{1}{12}\pi$	$\frac{5}{6}\pi$	$\frac{8}{3}\pi$	0.172	0.172
$\|0111\rangle$	$-\frac{5}{48}\pi$	$-\frac{5}{24}\pi$	$\frac{7}{12}\pi$	$\frac{13}{6}\pi$	0.028	0.028
$\|1000\rangle$	$-\frac{1}{6}\pi$	$\frac{2}{3}\pi$	$\frac{4}{3}\pi$	$\frac{8}{3}\pi$	0.012	0.012
$\|1001\rangle$	$-\frac{11}{48}\pi$	$\frac{13}{24}\pi$	$\frac{13}{12}\pi$	$\frac{13}{6}\pi$	0.007	0.007
$\|1010\rangle$	$-\frac{7}{24}\pi$	$\frac{5}{12}\pi$	$\frac{5}{6}\pi$	$\frac{8}{3}\pi$	0.005	0.005
$\|1011\rangle$	$-\frac{17}{48}\pi$	$\frac{7}{24}\pi$	$\frac{7}{12}\pi$	$\frac{13}{6}\pi$	0.004	0.004
$\|1100\rangle$	$-\frac{5}{12}\pi$	$\frac{1}{6}\pi$	$\frac{4}{3}\pi$	$\frac{8}{3}\pi$	0.003	0.003
$\|1101\rangle$	$-\frac{23}{48}\pi$	$\frac{1}{24}\pi$	$\frac{13}{12}\pi$	$\frac{13}{6}\pi$	0.003	0.003
$\|1110\rangle$	$-\frac{13}{24}\pi$	$-\frac{1}{12}\pi$	$\frac{5}{6}\pi$	$\frac{8}{3}\pi$	0.003	0.003
$\|1111\rangle$	$-\frac{29}{48}\pi$	$-\frac{5}{24}\pi$	$\frac{7}{12}\pi$	$\frac{13}{6}\pi$	0.003	0.003

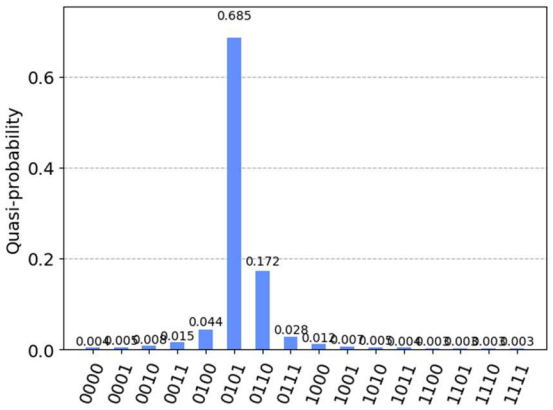

Figure 6 Qiskit Simulation Result of QPE Circuit for a Gate with Phase $\lambda = \frac{1}{3}$ USING 4 Measurement Qubits.

The probabilities are shown in the last column in Table 3, labeled as *simulated probability*. Table 3 confirms that the result of the simulation is consistent with the computed probability from our analysis.

Because $\frac{1}{3}$ is close to $\frac{5}{16}$, the probability of measuring $|y\rangle = |0101\rangle$ is highest and the probability decreases as the difference between y and $2^t\ \lambda$ increases, as it conforms to our intuition.

4. EVALUATION

Quantum phase estimation (QPE) is a vital component employed in many important quantum algorithms [16][17][18][19]. The ability to accurately estimate phase parameters is crucial for enabling quantum-enhanced computation in diverse fields ranging from cryptography [20][21][22][23] to material science [24][25][26].

In this paper, we have undertaken a comprehensive exploration of quantum phase estimation (QPE), focusing particularly on scenarios where the phase is not exactly represented as a rational number with a denominator in a power of 2. Through a rigorous mathematical analysis and precise computation of the quantum state of QPE in such cases, we have extended our understanding of this fundamental quantum algorithm.

Our analysis contributes to a deeper appreciation of the behavior of QPE and its applications. By leveraging insights from number theory and trigonometry, we have derived explicit expressions for the quantum state of QPE, providing valuable theoretical foundations for its practical implementation and optimization. In quantum chemistry and quantum simulation, where the phases represent energy eigenvalues or dynamics of quantum systems, exact or approximate computation of QPE enables accurate predictions of molecular properties, reaction rates, and material behavior. Similarly, in quantum machine learning and optimization, precise estimation of phases contributes to the development of efficient quantum algorithms for tasks like database search, pattern recognition, and optimization problems.

The validation of our theoretical results through simulations using the Qiskit framework underscores the accuracy and efficacy of our formulations. The comparison between theoretical predictions and Qiskit simulations serves as a testament to the reliability and utility of our approach, offering practitioners and researchers a reliable mathematical framework for analyzing QPE.

Moreover, our work contributes to the broader landscape of quantum computing research, highlighting the importance of understanding the behavior of fundamental quantum algorithms in various contexts. As quantum computing continues to evolve, with advancements in hardware, software, and algorithmic techniques, our insights into QPE pave the way for further innovation and exploration in the field.

In conclusion, this paper advances our understanding of quantum phase estimation and similar quantum operations, offering mathematical insights and rigorous formulation of quantum states.

REFERENCES:

[1] Kitaev, A.Y. Quantum measurements and the Abelian Stabilizer Problem, 1995, [arXiv:quant-ph/quant-ph/9511026].

[2] Shor, P.W. Algorithms for quantum computation: discrete logarithms and factoring. *Proceedings 35th Annual Symposium on Foundations of Computer Science* **1994**, pp. 124–134.

[3] Vandersypen, L.M.; Steffen, M.; Breyta, G.; Yannoni, C.S.; Sherwood, M.H.; Chuang, I.L. Experimental realization of Shor's quantum factoring algorithm using nuclear magnetic resonance. *Nature* **2001**, *414*, 883–887.

[4] Peng, X.; Liao, Z.; Xu, N.; Qin, G.; Zhou, X.; Suter, D.; Du, J. Quantum adiabatic algorithm for factorization and its experimental implementation. *Physical review letters* **2008**, *101*, 220405.

[5] Preskill, J. Quantum Computing in the NISQ era and beyond. *Quantum* **2018**, *2*, 79. doi:10.22331/q-2018-08-06-79.

[6] Rebentrost, P.; Gupt, B.; Bromley, T.R.; Weedbrook, C.; Lloyd, S. Quantum computational finance: Monte Carlo pricing of financial derivatives. *Physical Review A* **2018**, *98*, 022321.

[7] Moll, N.; Barkoutsos, P.K.; Egger, D.J.; Sørensen, J.J.W.H.; Demler, E.; Troyer, M. Quantum optimization using variational algorithms on near-term quantum devices. *Quantum Science and Technology* **2018**, *3*, 030503.

[8] Cleve, R.; Ekert, A.; Macchiavello, C.; Mosca, M. Quantum algorithms revisited. *Proceedings of the Royal Society of London. Series A: Mathematical, Physical and Engineering Sciences* **1998**, *454*, 339–354.

[9] Mohammadbagherpoor, H.; Oh, Y.H.; Dreher, P.; Singh, A.; Yu, X.; Rindos, A.J. An Improved Implementation Approach for Quantum Phase Estimation on Quantum Computers. 2019 IEEE International Conference on Rebooting Computing (ICRC), 2019, pp. 1–9. doi:10.1109/ICRC.2019.8914702.

[10] Wille, R.; Van Meter, R.; Naveh, Y. IBM's Qiskit Tool Chain: Working with and Developing for Real Quantum Computers. 2019 Design, Automation & Test in Europe Conference & Exhibition (DATE), 2019, pp. 1234–1240. doi:10.23919/DATE.2019.8715261.

[11] Dirac, P.A.M. *The Principles of Quantum Mechanics*; Oxford University Press, 1958.

[12] Nielsen, M.A.; Chuang, I.L. *Quantum computation and quantum information*; Cambridge university press, 2010.

[13] Hales, L.; Hallgren, S. An improved quantum Fourier transform algorithm and applications. *Proceedings 41st Annual Symposium on Foundations of Computer Science*, 2000, pp. 515–525. doi:10.1109/SFCS.2000.892139.

[14] Fowler, A.G.; Mariantoni, M.; Martinis, J.M.; Cleland, A.N. Surface codes: Towards practical large-scale quantum computation. *Phys. Rev. A* **2012**, *86*, 032324. doi:10.1103/PhysRevA.86.032324.

[15] LaRose, R. Overview and Comparison of Gate Level Quantum Software Platforms. *Quantum* **2019**, *3*, 130. doi:10.22331/q-2019-03-25-130.

[16] Wang, Y.; Zhang, L.; Yu, Z.; Wang, X. Quantum phase processing and its applications in estimating phase and entropies. *Phys. Rev. A* **2023**, *108*, 062413. doi:10.1103/PhysRevA.108.062413.

[17] Ouedrhiri, O.; Banouar, O.; Hadaj, S.E.; Raghay, S. Quantum phase estimation based algorithms for machine learning. *2021 2nd International Informatics and Software Engineering Conference (IISEC)*, 2021, pp. 1–6. doi:10.1109/IISEC54230.2021.9672406.

[18] Harrow, A.W.; Hassidim, A.; Lloyd, S. Quantum Algorithm for Linear Systems of Equations. *Phys. Rev. Lett.* **2009**, *103*, 150502. doi:10.1103/PhysRevLett.103.150502.

[19] Montanaro, A. Quantum algorithms: An overview. *npj Quantum Information* **2015**, *2*. doi:10.1038/npjqi.2015.23.

[20] Gisin, N.; Ribordy, G.; Tittel, W.; Zbinden, H. Quantum cryptography. *Rev. Mod. Phys.* **2002**, *74*, 145–195. doi:10.1103/RevModPhys.74.145.

[21] Rivest, R.L.; Shamir, A.; Adleman, L.M. A method for obtaining digital signatures and public-key cryptosystems. *Communications of the ACM* **1978**, *21*, 120–126.

[22] Bennett, C.H.; Brassard, G. Quantum cryptography: Public key distribution and coin tossing. *Theoretical Computer Science* **2014**, *560*, 7–11. Theoretical Aspects of Quantum Cryptography – celebrating 30 years of BB84, doi:https://doi.org/10.1016/j.tcs.2014.05.025.

[23] Elliott, C.; Pearson, D.; Troxel, G. Quantum cryptography in practice. *Proceedings of the 2003 Conference on Applications, Technologies, Architectures, and Protocols for Computer Communications*; Association for Computing Machinery: New York, NY, USA, 2003; SIGCOMM '03, p. 227–238. doi:10.1145/863955.863982.

[24] Kang, C.; Bauman, N.P.; Krishnamoorthy, S.; Kowalski, K. Optimized Quantum Phase Estimation for Simulating Electronic States in Various Energy Regimes. *Journal of Chemical Theory and Computation* **2022**, *18*, 6567–6576. doi:10.1021/acs.jctc.2c00577.

[25] Cao, Y.; Romero, J.; Olson, J.P.; Degroote, M.; Johnson, P.D.; Kieferová, M.; Kivlichan, I.D.; Menke, T.; Peropadre, B.; Sawaya, N.P.D.; others. Quantum chemistry in the age of quantum computing. *Chemical reviews* **2019**, *119*, 10856–10915.

[26] Babbush, R.; Huggins, W.; Berry, D.; Ung, S.; Zhao, A.; Reichman, D.; Neven, H.; Baczewski, A.; Lee, J. Quantum simu- lation of exact electron dynamics can be more efficient than classical mean-field methods. *Nature Communications* **2023**, *14*. doi:10.1038/s41467-023-39024-0.